ELSEVIER

Polymer 41 (2000) 4089–4097

polymer

Specific features of the interfacial tension in the case of phase separated solutions of random copolymers

A. Schneider[a,b], B.A. Wolf[a,b,*]

[a]*Institut für Physikalische Chemie, Johannes Gutenberg-Universität, Jakob-Welder-Weg 13, 55099 Mainz, Germany*
[b]*Materialwissenschaftliches Forschungszentrum der Universität, D-55099 Mainz, Germany*

Received 27 April 1999; received in revised form 5 August 1999; accepted 19 August 1999

Abstract

Phase diagrams (cloud point curves, critical points, tie lines for constant critical composition) and interfacial tensions as a function of temperature were measured for solutions of two random copolymers: poly(dimethylsiloxane-*ran*-methylphenylsiloxane) [I] and poly(styrene-*ran*-acrylonitrile) [II]. Acetone and anisole served as solvents for I and toluene for II; all solutions exhibit UCSTs between 300 and 310 K. The phase separation behavior can be well modeled if one accounts for the molecular and chemical non-uniformities of the random copolymers used in this study. The interfacial tensions σ differ most markedly from that of comparable homopolymer solutions in their correlation $\sigma = \sigma_\tau \tau^\mu$, where $\tau = (T_c - T)/T_c$. For all three systems σ_τ results considerably less and the critical exponent μ varies widely from 0.68 to 2.18 (in contrast to the normal case where μ is on the order of 1.3–1.5). Both observations are explained in terms of the capability of copolymers to minimize the interfacial energy by suitably arranging their different monomeric units. Model calculations were performed in terms of the energy required to transfer molecules from one phase to the other, assembling the average polymer–solvent interaction parameter from the three binary interaction parameters g_{ij}, required to describe copolymer solutions. These results demonstrate that the experimentally observed particularities of copolymers are more likely dominated by dissimilarities in the concentration dependence of g_{ij} than by unlike temperature dependencies. Particularities in the correlations of the length of the tie line with τ and σ, respectively, are also discussed.

Keywords: Random copolymer solutions; Interfacial tension; Phase diagrams

1. Introduction

The present investigation was undertaken with the primary objective of checking whether the interfacial properties of demixed copolymer solutions differ fundamentally from that of homopolymer solutions. In view of the fact that the thermodynamic variability should be much larger in the case of macromolecules consisting of two different types of mers. In terms of interactions between the different kinds of segments (fixed in their size by the volume of the solvent) three interaction parameters are required to define the system instead of one. It is therefore not far-fetched to expect dissimilarities.

Unlike numerous studies concerning the demixing and the interfacial behavior of phase separated homopolymer solutions we were unable to find similar work for random copolymers in the literature. One possible reason is the fact that molecularly uniform copolymers are not readily available. Research in this area is therefore complicated by the necessity to account not only for the distribution of molar masses but also for that of chemical composition. In the present work we have dealt with that problem in terms of continuous thermodynamics. Furthermore we have made all interfacial measurements with solutions of over-all critical composition since the coexistence curve is only uninterrupted under that condition and one can study experimentally how σ approaches zero as T moves towards T_c (for a more detailed discussion confer Ref. [1]).

2. Experimental

2.1. Materials

The random copolymer poly(dimethylsiloxane-*ran*-methylphenylsiloxane) P($DMS_{0.9}$-*ran*-$MPS_{0.1}$)41w was polymerized anionically and purchased from Dow Corning Corporation (Midland, USA; commercial name: 510 Fluid 500 cSt). M_w (41 kg/mol) and M_n (9 kg/mol) have been

* Corresponding author. Address: Institut für Physikalische Chemie, Johannes Gutenberg-Universität, Mainz. Tel.: +49-6131-39-2491; fax: +49-6131-39-4640.

E-mail address: bernhard.wolf@uni-mainz.de (B.A. Wolf).

0032-3861/00/$ - see front matter
PII: S0032-3861(99)00643-6

Nomenclature

$\overline{\overline{\Delta G}}^R$	residual segment molar Gibbs energy of mixing (Eq. (5))
$\overline{\overline{\Delta G}}$	segment-molar Gibbs energy of mixing (Eq. (1))
f	volume fraction of A segments contained in the copolymer
g_{ij}	interaction parameter referring to segments i and j
k	$1/(M_w/M_n - 1)$
M	molar mass
N	number of segments a copolymer contains
V	molar volume
X	number of monomeric units a copolymer contains
y	weight fraction of less abundant monomeric unit in a copolymer species
$\hat{y}$	average weight fraction of less abundant monomeric unit
Greek symbols	
$\Delta\varphi$	length of tie line
β_s	critical exponent (Eq. (8))
ε	hump energy
ε_{cd}	parameter, measuring the width of the chemical distribution
μ	critical exponent (Eq. (10))
σ	interfacial tension
τ	reduced temperature $= (T_c - T)/T_c$
ϕ	critical exponent (Eq. (21))
φ	segment-mole fraction
ζ	critical exponent (Eq. (20))
Subscripts	
1	solvent
2 or p	copolymer
o	momomer
c	critical
n	number average
w	weight average
A, B	type of monomer
Superscripts	
*	hard core
Adjustable parameter	
A, *AA*, *B*, *BB*	Eq. (22)
c, *d*	Eq. (6)
β_0, β_1	Eq. (7)
β_{1A}, β_{1B}, p_{1A}, p_{1B}	Eq. (23)
γ_{1A}, γ_2	Eq. (5)

determined by GPC (PDMS-standards and universal calibration). The content of MPS (10%) was measured by NMR spectroscopy. Poly(styrene-*ran*-acrylonitrile) P($S_{0.6}$-*ran*-$AN_{0.4}$) 147w stems from BASF (Ludwigshafen, Germany). It is also a random copolymer and contains 40% AN. M_w is according to light scattering in tetrahydrofurane (THF) 147 kg/mol, M_n from osmotic pressure measurements in THF amounts to 90 kg/mol. PDMS 24.5w is a product of Wacker GmbH (Muenchen, Germany; trade name: PDMS AK350) with $M_w = 24.5$ kg/mol and $M_n = 11$ kg/mol, as determined by GPC. Phenetole (PTL), anisole (ANL), toluene (TL), and acetone (AC) were dried over molecular sieves before use.

2.2. Procedures

Cloud point curves and interfacial tensions (spinning-drop method) were determined as already described in Ref. [2].

Critical points: these data were obtained from phase volume ratios. In this method [3] homogeneous solutions of different polymer concentrations are cooled as little as possible below their cloud point to excrete a macroscopically sizeable second phase. The phase volumes are then determined and the logarithm of the phase volume ratio is plotted as a function of composition. From the straight lines obtained one can read the critical concentration from the

condition of equal volume of the coexisting phases irrespective of the shape of the cloud point curve.

Tie lines: polymer solutions of critical composition were slowly cooled from the homogeneous region to a temperature where the liquid demixes. After completion of macroscopic phase separation (typically requiring one to two days) adequate amounts of each of the totally clear coexisting phases were taken by means of a syringe and weighted. The composition of these liquids was then determined by evaporation of the solvent and weighting of the remaining polymer. In order to check for possible fractionation with respect to chemical composition, the polymers were also analyzed by NMR.

3. Theoretical background

3.1. Phase diagram

In order to account for molecularly or/and chemically non-uniform polymers, phase equilibria of the polymer solutions are often described by means of continuous thermodynamics, a method using continuous distribution functions [4,5].

For the present solutions of random copolymers, consisting of two types of monomeric units, the segment-molar Gibbs free energy $\overline{\overline{\Delta G}}/RT$ is given by Eq. (1)

$$\frac{\overline{\overline{\Delta G}}}{RT} = \frac{1-\varphi_2}{N_1} + \int_{N_{2,u}}^{N_{2,o}} \int_{y=0}^{y=1} \frac{\varphi_2 W(N_2,y)}{N_2} \ln \varphi_2 W(N_2,y)\, dy\, dN_2 + \overline{\overline{\Delta G}}^R \quad (1)$$

φ_2 is the segment-mole fraction of the copolymer in the solution, N_1 and N_2 are the segment numbers of solvent and copolymer, respectively, and $\overline{\overline{\Delta G}}^R$ is the residual segment molar Gibbs free energy of the system. To account for the two possible types of polydispersity (chain length and copolymer composition) we use the divariant distribution function $W(N_2,y)$ proposed by Stockmayer [6]

$$W(N_2,y) = \left[\frac{k^{k+1}}{N_{2,n}\Gamma(k+1)} \left(\frac{N_2}{N_{2,n}}\right)^{k+1} \exp\left(-k\frac{N_2}{N_{2,n}}\right)\right] \times \left[\sqrt{\frac{N_2}{2\pi\varepsilon_{cd}}} \exp - \frac{N_2(y-\hat{y})^2}{2\varepsilon_{cd}}\right] \quad (2)$$

The first part of Eq. (2) corresponds to a generalized Schulz–Flory function. $N_{2,n}$ is the number average of the segment numbers calculated from the number average of the molecular volume of the copolymer using the van-der-Waals volume of the different monomers, weighted by the chemical composition and normalized to the van-der-Waals volume of the solvent. The parameter k is defined as

$$k = \left(\frac{M_w}{M_n} - 1\right)^{-1} \quad (3)$$

and Γ constitutes the gamma function frequently used in statistics. The second part of Eq. (2) constitutes a Gaussian distribution of the chemical composition (mass fraction y of the minor component of a certain polymer species) around $\hat{y}$, the average chemical composition of a random copolymer consisting of X_A units of type A and X_B units of type B defined as

$$\hat{y} = \frac{X_B M_{o,B}}{X_A M_{o,A} + X_B M_{o,B}} \quad (4)$$

and ε_{cd} measures the width of the Gaussian distribution.

The segment molar residual Gibbs free energy of the system, $\overline{\overline{\Delta G}}^R$, is modeled as described in Ref. [4]

$$\frac{\overline{\overline{\Delta G}}^R}{RT} = L(\varphi_2)\chi(T)(1 + \gamma_1\hat{y} + \gamma_2\hat{y}^2) \quad (5)$$

with

$$L(\varphi_2) = \varphi_2(1-\varphi_2)(1 + c\varphi_2 + d\varphi_2^2) \quad (6)$$

and

$$\chi(T) = \beta_0 + \frac{\beta_1}{T} \quad (7)$$

where γ_1 and γ_2 measure the influences of chemical composition on $\overline{\overline{\Delta G}}^R$ and $L(\varphi_2)$ describes its concentration dependence by means of the two empirical parameters c and d. Temperature influences are given by β_0 and β_1.

Cloud point curves are according to theory defined as the boundary between the homogeneous and the heterogeneous region of a system. The amount of matter contained into the segregated phase ($''$) at the cloud point temperature is so insignificant that the composition of the main phase ($'$) can be considered to be identical with that of the starting solution. Conversely the composition of the infinitely small amounts of the first secreted minor phases yield shadow curves.

Spinodal curves and critical points are calculated from continuous thermodynamics [7–10]. They are determined by means of the two additional equations resulting form the condition that the second (spinodal) and the second plus third (critical point) derivatives of the segment-molar Gibbs free energy (Eq. (1)) with respect to composition (in the actual case φ_2) become zero.

3.2. Interfacial tension

The following relations should hold true for near critical conditions [11]. The length $\Delta\varphi$ of the tie line is related to the relative distance to the critical temperature, $\tau = (T_c - T)/T_c$, according to Eq. (8). The interfacial tension σ as a function of $\Delta\varphi$ is given by Eq. (9) and the

Table 1
Values of the critical exponents [11,14] resulting from mean-field theory and Ising model

	Mean-field theory	Ising model
β_s	0.5	0.32
μ	1.5	1.26
μ/β_s	3.0	3.88

interrelation between σ and τ by Eq. (10)

$$\Delta\varphi = \Delta\varphi_\tau(\tau)^{\beta_s} \tag{8}$$

$$\sigma = \sigma_{\Delta\varphi}(\Delta\varphi)^{\mu/\beta_s} \tag{9}$$

$$\sigma = \sigma_\tau \tau^{\mu} \tag{10}$$

The values of the critical exponents β_s and μ, resulting from the mean-field theory [12–14] and from the Ising model [15] are collected in Table 1.

4. Results and discussion

4.1. Phase diagrams

Cloud point curves and critical points of the systems AC/P($DMS_{0.9}$-*ran*-$MPS_{0.1}$) 41w, ANL/P($DMS_{0.9}$-*ran*-$MPS_{0.1}$) 41w and TL/P($S_{0.6}$-*ran*-$AN_{0.4}$) 147w have been measured as described. In order to calculate their phase diagrams, N_1, the number of segments the solvent consists of, and the parameters $N_{2,n}$, $\hat{y}$, k and ε_{cd}, characterizing the copolymer, have to be known. In all cases N_1 was set equal to unity and the hard-core volume, as calculated from the van der Waals increments reported by Bondi [16] and Gottlieb [17], was taken as the segmental volume.

For the copolymer we introduce a hypothetical (averaged) monomeric unit and calculate its a hard-core volume according to

$$V^*_{o,2} = \frac{X_A}{X_A + X_B} V^*_{o,A} + \frac{X_B}{X_A + X_B} V^*_{o,B} \tag{11}$$

with the molar mass $M_{o,2}$

$$M_{o,2} = \frac{X_A}{X_A + X_B} M_{o,A} + \frac{X_B}{X_A + X_B} M_{o,B} \tag{12}$$

$N_{2,n}$, the number of hard-core segments of the copolymer, can then be calculated from the number average molar mass of the copolymer, as obtained from GPC, by means of the relations

$$V^*_2 = M_n(\mathrm{GPC}) \frac{V^*_{o,2}}{M_{o,2}} \tag{13}$$

and

$$N_{2,n} = \frac{V^*_2}{V^*_1} \tag{14}$$

AC/P(DMS0.9-ran-MPS0.1) 41w: the molar hard-core volume of AC is 43.54 cm^3/mole. The molar volume of the "mixed" monomeric unit of the copolymer is $V^*_{o,2}$ = 47.31 cm^3/mol and its molar mass $M_{o,2}$ = 80.2 g/mol. The molar volume of the present copolymer results to 5368 cm^3/mol yielding $N_{2,n}$ = 123.3. The mass average chemical composition $\hat{y}$ amounts to 0.15 and k = 0.286. The chemical non-uniformity, quantified by ε_{cd}, could in principle be calculated from the kinetic parameters of the copolymerization [4]. Since this information was unavailable we have set ε_{cd} = 0.25, a value which is typical for a random copolymer [4].

Eq. (5) contains six parameters: two (β_0, β_1) for the temperature dependence of the residual segment molar Gibbs energy of mixing, two (c, d) for its variation with concentration and two (γ_1, γ_2) to quantify the influence of the chemical composition of the copolymer. Not all of them are, however, required to model the measured cloud point curve of the present system. It suffices to account either for the concentration-dependence or for the dependence on chemical composition.

Fig. 1 shows the experimental cloud points and tie lines in comparison to the cloud point curve and shadow curve calculated by means of the following parameters

$$\beta_0 = -0.62; \qquad \beta_1 = 278.9\ \mathrm{K}; \qquad \gamma_1 = 4.169; \qquad \gamma_2 = c = d = 0 \tag{15}$$

where these values were obtained by adjusting such that they fit the experimental results best. The fact that the critical point is—in contrast to truly binary systems—not situated in the maximum of the cloud point curve but shifted towards higher polymer concentration is well know and reflects the non-uniformity of the copolymer. Similarly one branch of the coexistence curve (for critical over-all

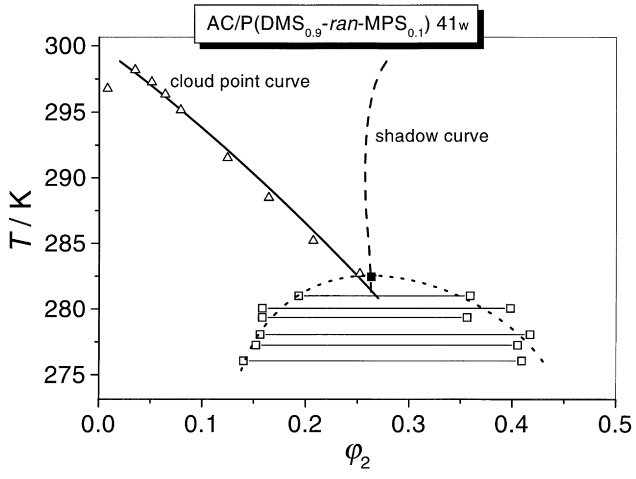

Fig. 1. Phase diagram of the system AC/P($DMS_{0.9}$-*ran*-$MPS_{0.1}$) 41w. Cloud points (triangles), tie lines (for constant critical over-all concentration, the dotted line is just a guide for the eye) and the critical point (full square) represent experimental data. The full line gives the calculated cloud point curve and the dashed line the corresponding shadow curve.

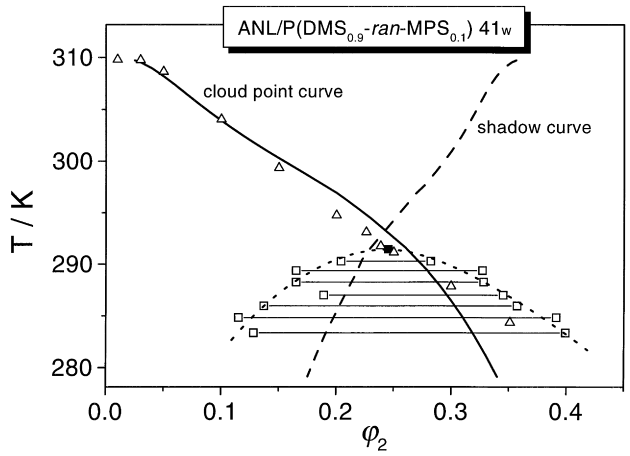

Fig. 2. As Fig. 1 but for the system ANL/P($DMS_{0.9}$-*ran*-$MPS_{0.1}$) 41w.

composition) is located inside and the other one outside the area defined by the cloud point curve due to polymer fractionation associated with phase separation.

ANL/P(DMS0.9-ran-MPS0.1)41w: the hard-core volume of ANL amounts to 62.7 cm^3/mol. The polymer is identical with the last example but the larger solvent leads to a smaller value of $N_{2,n} = 85.6$. For this system we give an example for the equivalence of adjusting γ_1 and γ_2 (Eq. (5)) and setting $c = d = 0$ (Eq. (6)) with the opposite procedure. The measured cloud point curve can either be modeled by:

$$\beta_0 = -0.62; \qquad \beta_1 = 291\ \text{K}; \qquad \gamma_1 = 3.99; \qquad \gamma_2 = c = d = 0 \tag{16}$$

or

$$\beta_0 = 0.74; \qquad \beta_1 = 18.35\ \text{K}; \qquad \gamma_1 = \gamma_2 = 0; \qquad c = 0.352; \qquad d = 0.2 \tag{17}$$

Fig. 2 shows the results for Eq. (17).

TL/P(S0.6-ran-AN0.4): the hard-core volume of TL is 59.5 cm^3/mol, the value for the average copolymer segment

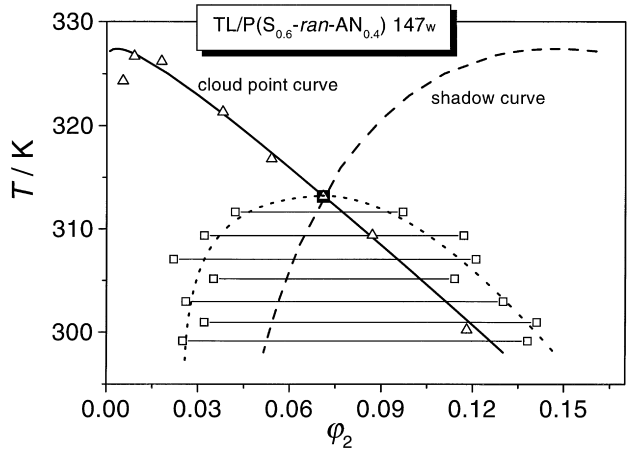

Fig. 3. As Fig. 1 but for the system TL/P($S_{0.6}$-*ran*-$AN_{0.4}$) 147w.

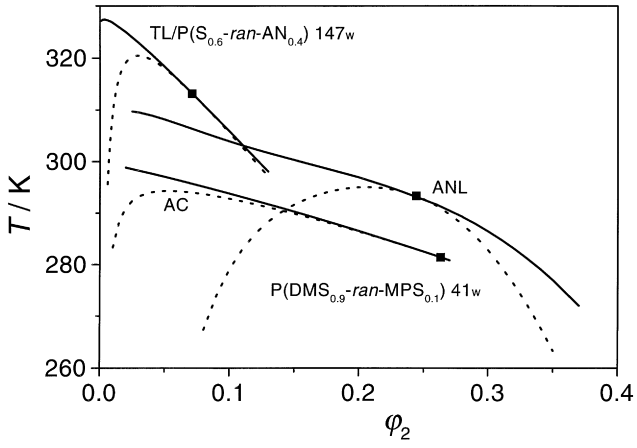

Fig. 4. Comparison of the phase diagrams of the three copolymer solutions under consideration as modeled by means of the measured cloud point curves and critical compositions.

reads 50.4 cm^3/mol. By means of the corresponding average mass of the segment 83.6 g/mol one obtains $N_{2,n} = 921.78$. The copolymer is characterized by $\hat{y} = 0.25$, $k = 1.515$ and $\varepsilon_{cd} = 0.25$. The parameter set used for the calculations shown in Fig. 3 is

$$\beta_0 = 0.05; \qquad \beta_1 = 61.28\ \text{K}; \qquad \gamma_1 = 4.65; \qquad \gamma_2, c, d = 0 \tag{18}$$

Cloud point curves and spinodals plus critical conditions calculated on the basis of the above equations for the three copolymer solutions under consideration are compared in Fig. 4. Reasonable agreement between calculated and experimental cloud point curves can be achieved in all cases, accounting for the distribution of chain lengths via Eq. (2), regardless of whether either the influences of chemical composition or the concentration-dependence is neglected in the computation of $\overline{\overline{\Delta G^R}}/RT$. Since the analysis of the copolymers contained in the coexisting phases by means of NMR did not yield any indication for fractionation according to the chemical composition, the latter variant appears more realistic. However, it requires four parameters to model the phase diagrams (β_0, β_1, c and d), in contrast to the former alternative which needs only three (β_0, β_1 and γ_1).

The shift of the critical composition out of the maxima of the cloud point curves towards higher polymer concentration results from the polydispersities of the present polymers and is in accord with experimental experience. The much lower critical polymer concentration observed for the system TL/P($S_{0.6}$-*ran*-$AN_{0.4}$) 147w as compared with that of solutions of P($DMS_{0.9}$-*ran*-$MPS_{0.1}$) 41w is due to the differences in the molar masses of the polymer. An analogous explanation for the disparity of the critical compositions for AC and ANL does, however, not hold true, since the number of segments calculated for P($DMS_{0.9}$-*ran*-$MPS_{0.1}$) 41w from the molar volume of AC is more than

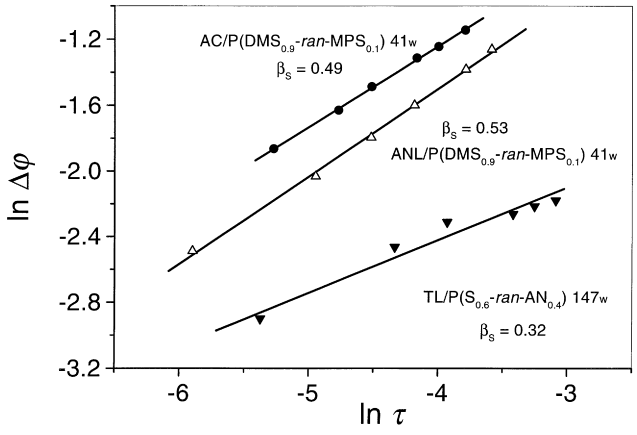

Fig. 5. Correlation between $\Delta\varphi$, the length of the tie lines, and $\tau = (T_c - T)/T_c$, the relative distance of T to the critical temperature. The $\Delta\varphi$ values were read from the coexisting curves shown in the phase diagrams (dotted lines in Figs. 1–3).

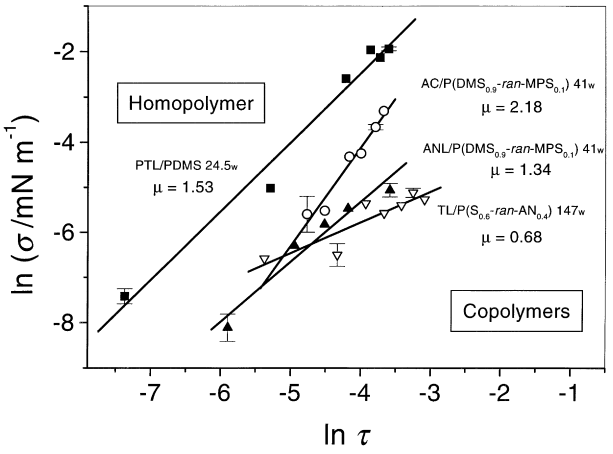

Fig. 7. Correlation between σ and τ according to Eq. (10). For comparison such a dependence is also shown for a typical homopolymer solution.

40% larger than in the case of ANL and yet the critical point is higher for AC.

4.2. Interfacial tension

Interfacial tensions were exclusively measured for critical over-all compositions of the copolymer solutions. Data analysis with respect to critical exponents starts with diagrams relating the length of the tie lines, $\Delta\varphi$, and τ, the relative temperature distance to T_c (Fig. 5, Eq. (8)). Then we investigate the interrelation of σ and $\Delta\varphi$ (Fig. 6, Eq. (9)). Finally, it is examined whether the dependencies of σ on τ observed with the present copolymer systems, exhibit special features as compared with homopolymer solutions (Fig. 7, Eq. (10)). In order to eliminate some of the experimental errors in the length of the tie lines, we use the data read from the smooth coexistence curves of Figs. 1–3 for the following evaluation.

The critical exponents (β_s) of the siloxane-copolymer containing systems show good agreement with the value

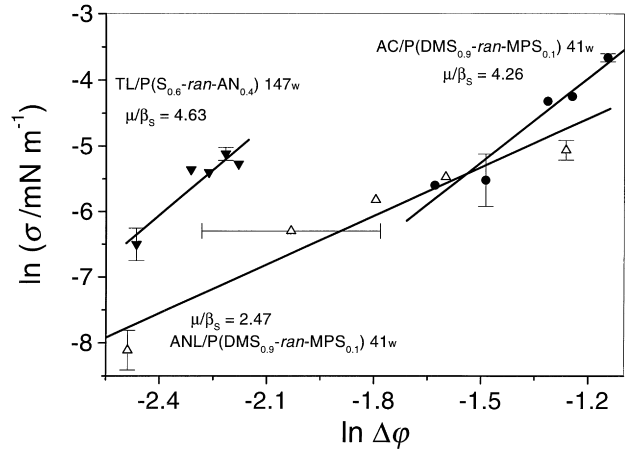

Fig. 6. Correlation between σ and $\Delta\varphi$ according to Eq. (9).

predicted by the mean-field-theory in contrast to the behavior of TL/P(S-*ran*-AN) which is better described by the Ising model [15] (cf. Table 1). The observed approximately parallel displacement of the lines, corresponding to different $\Delta\varphi_\tau$ values in Eq. (8), should reflect the heats of mixing of the systems. This consideration can be rationalized by the fact that a given constant penetration into the two-phase regime in terms of constant $\tau = (T_c - T)/T_c$ does not fix the solvent quality as expressed by the length of the tie line. On the basis of the lattice theory one can calculate a generalized phase diagram in which the Flory–Huggins interaction parameter g replaces T. How this phase diagram turn into a real case depends on the temperature dependence of g, i.e. reflects the heat of mixing.

These considerations can be directly checked by means of the binodals (coexistence curves) for critical over-all concentrations of the systems shown in Figs. 1–3. According to that information the heat of mixing is much smaller for the system TL/P(S-*ran*-AN) than for the other two copolymer solutions for which the enthalpy effects are comparable. This result is in agreement with the relative position of the lines in Fig. 5. With the solvent TL one requires much larger τ values to realize a certain length of the tie line $\Delta\varphi$ than with AC or ANL.

Fig. 6 shows the dependence of interfacial tension σ on the length of tie lines according to Eq. (9). In contrast to β_s the ratio μ/β_s resulting from the present evaluation can neither be described by the mean-field theory, nor by the Ising model. For TL/P(S-*ran*-AN) and AC/P(DMS-*ran*-MPS) the values are considerably too high and for ANL/P(DMS-*ran*-MPS) it is too low (cf. Table 1). In the assessment of this result it must, however, be borne in mind that the experimental errors lead to the largest uncertainty in the critical exponents.

Fig. 7 deals with the correlation between σ and reduced temperature τ as described by Eq. (10). The diagram shows a comparison between the three-copolymer systems and the homopolymer system PTL/PDMS 24.5w. The most striking

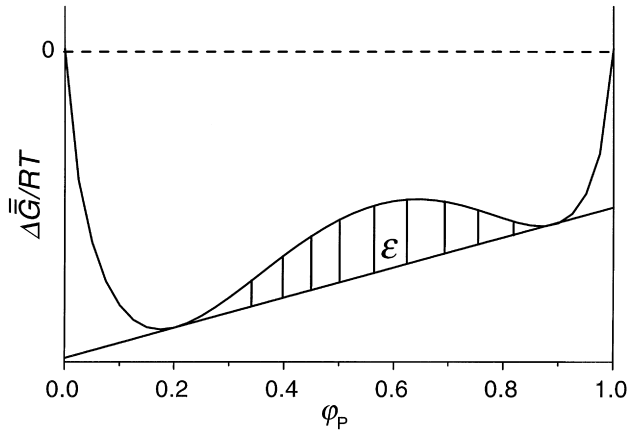

Fig. 8. Scheme illustrating how the reduced hump energy ε is calculated from the variation of $\bar{\bar{G}}$, the segment molar Gibbs energy of mixing, with φ_2, the volume fraction of polymer.

observation consists in the fact that the interfacial tensions of the copolymer solutions are in all three cases lower (up to a factor of 0.1) than those of the homopolymer system for a given reduced temperature. This observation can be understood in terms of phenomenological thermodynamics by the additional degree of freedom of copolymers as compared with homopolymers to arrange the segments in the interphase between the two coexisting bulk phases. The monomeric unit interacting more favorably with the solvent will accumulate at the interface adjacent to the dilute solution to the extent the entropy cost permits it. This situation leads to an additional reduction of the Gibbs energy of the interfacial layer.

In addition to the already discussed shift of the interrelation between σ and τ to lower σ values one also observes characteristic differences in the critical exponent μ. With ANL/P(DMS-*ran*-MPS) the value lies between the prediction of the mean-field theory (1.5) and the Ising model (1.26). For AC/P(DMS-*ran*-MPS) the observed $\mu = 2.18$ exceeds these values considerably, whereas $\mu = 0.68$ for TL/P(S-*ran*-AN) remains well below the forecasts. In the next section we present some model calculations performed to rationalize the present findings.

4.3. Model calculations

So far all thermodynamic considerations were based on continuous thermodynamics which starts from the residual Gibbs energy of mixing and does not use Flory–Huggins interaction parameters between the three different species of the present systems explicitly. Since it appears obvious that the particularities of random copolymers made of A and B units as compared with homopolymers should result from the fact that three of these parameters are required to describe copolymer solutions of the present type, we introduce the composed interaction parameter g_{1P} between the solvent 1 and the "averaged" copolymer P according to the following relation [18] for the subsequent discussion:

$$g_{1P} = f \cdot g_{1A} + (1 - f) \cdot g_{1B} - f(1 - f) g_{AB} \tag{19}$$

where f is the volume fraction of A segments contained in the copolymer.

Furthermore we make use of two additional scaling laws formulated for the reduced hump energy ε [19,20] (for its definition confer Fig. 8). That quantity is given by the area located between the composition dependence of the Gibbs energy of the *homogeneous* system and the double tangent to this function and constitutes a measure for the energy required transferring molecules from one coexisting phase to the other. These relations read

$$\varepsilon = \varepsilon_\tau \tau^\zeta \tag{20}$$

$$\sigma = \sigma_\varepsilon \varepsilon^\phi \tag{21}$$

Since molecular or chemical non-uniformities of the copolymers should not change the principal features, the model calculations are restricted to a truly binary system. The interaction parameters of Eq. (19) where on the other hand chosen as close to reality as possible by adjusting them to the measured cloud point curve for the systems AC/PDMS [21] and AC/P(DMS-*ran*-MPS) (cf. Fig. 1). For that purpose the precipitation threshold was taken as the critical point. The number of segments of PDMS was set $N_{PDMS} = 404$ and $N_{P(DMS\text{-}ran\text{-}MPS)} = 123.3$ and $f = 0.9$ chosen identical with the values used in the previous section. The results demonstrate that the last term of Eq. (19) can be neglected as compared with the first two summands.

By means of the subsequent model calculations we want to check the validity of the hypothesis that the dissimilarities in the behavior of copolymers A-*ran*-B and of homopolymers should be due to the fact that g_{1P} is composed of three interaction parameters, which may vary with temperature or/and composition in very different ways. Since we do not know of any reliable possibilities for a direct theoretical predictions of σ from the knowledge of temperature and composition dependent interaction parameters we base the subsequent considerations on hump energies [19] which are directly related to σ.

Different temperature dependencies: The following simplified expression (neglect of g_{AB}) was used to describe the copolymer:

$$g_{1P} = f(A + AA/T) + (1 - f)(B + BB \cdot T) \tag{22}$$

The parameters *A* and *AA*, characterizing the homopolymer A, known from vapor pressure measurements [21], were slightly changed to yield the critical data. The effects of a variation of *B* and *BB*, accounting for the contributions of the comonomeric units B, are given in Fig. 9 which shows the results of such calculations in terms of the correlation between ε and τ (Eq. (20)).

The critical exponent of the solvent homopolymer system ($\zeta = 2.56$) is in good agreement with mean-field theory

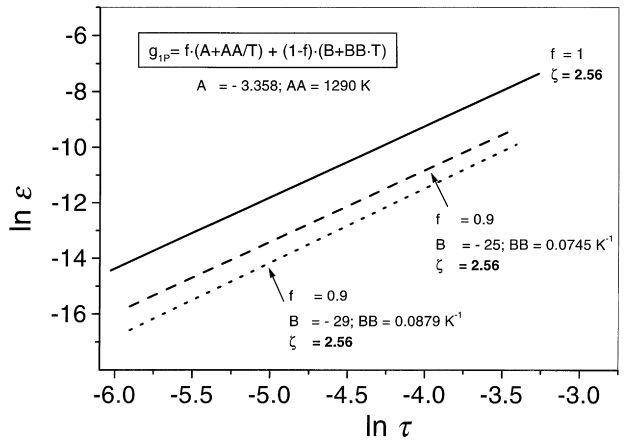

Fig. 9. Correlation between the reduced hump energy ε and τ according to Eq. (20). The curves are computed for a model system under the assumption that the temperature dependence of the interaction parameter between the solvent and the two different mers is very dissimilar (g_{1P} of Eq. (22)).

($\zeta = 2.5$, Ising-model: $\zeta = 2.22$). In order to create smaller ε values for the copolymer (corresponding to the experimentally observed lower σ of copolymer solutions) it is necessary to chose B highly negative. The slopes of these lines in Fig. 9, however, remain unchanged. It appears therefore unlikely that the experimentally observed changes in μ are primarily due to differences in the temperature dependence of the interaction parameters between the solvent and the two kinds of monomeric units.

Different concentration dependencies: these calculations were performed modeling the concentration dependence in the binary interaction parameters g_{1A} and g_{1B} according to Enders [19]

$$g_{1P} = f\cdot\beta_{1A}\frac{(1-p_{1A})}{T(1-p_{1A}\cdot f\cdot\varphi_p)} + (1-f)\beta_{1B}\frac{(1-p_{1B})}{T(1-p_{1B}\cdot(1-f)\cdot\varphi_P)} \quad (23)$$

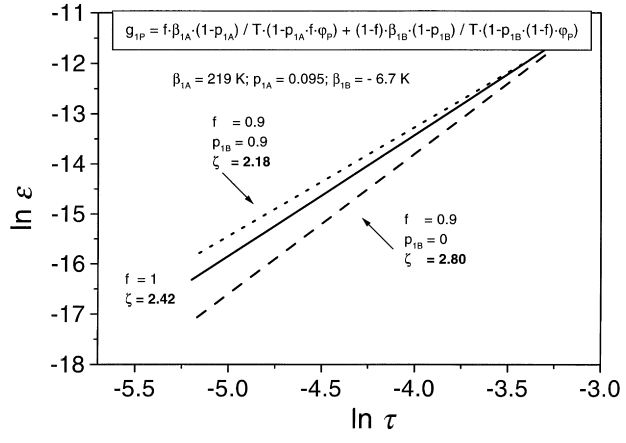

Fig. 10. As Fig. 9 but assuming largely different concentration dependencies of these interaction parameters (g_{1P} of Eq. (23)).

where β_{1A} and p_{1A} were chosen such that they reproduce the critical data of the homopolymer A and yield $\zeta = 2.42$ (a value between the mean-field and the Ising prediction). The parameters β_{1B} and p_{1B}—characterizing the contribution of the comonomer B—were then varied conjointly to maintain the critical point. The results of these computations for the parameters indicated in the graph can be seen from Fig. 10.

The outcome demonstrates that dissimilar composition dependencies of the interaction parameters between the solvent and the two monomeric units may indeed not only shift the interrelation of ln ε and ln τ in an approximately parallel manner, but that they can also change the critical exponent ζ (corresponding to the experimentally determined μ) markedly.

5. Conclusions

The present experimental results clearly demonstrate pronounced differences in the interfacial properties of demixed copolymer solutions as compared with demixed homopolymer solutions. For given depth of penetration into the two phase regime (constant τ) and critical overall composition the interfacial tension results much lower in the case of copolymers and some critical exponents vary within much wider limits. Both observations can be rationalized in terms of the additional possibilities of copolymers to arrange themselves within the interphase such that the Gibbs energy becomes even smaller. Model calculations performed to quantify these effects indicate that there exist at least two options to account for the additional features, namely dissimilar dependencies of the interaction parameters between the solvent and the two types of mers on temperature and composition. According to the present computations the former possibility acts primarily towards a reduction of σ whereas the latter also influences the critical exponents.

The differences in the behavior of copolymers and homopolymers were found to be much more pronounced in the case of $\sigma(\tau)$ than for $\sigma(\Delta\varphi)$. This observation constitutes an additional argument for the utilization of the length of the tie line instead of the reduced temperature distance to the critical point for the prediction of interfacial tensions. The advantage of that preference has already become very obvious with solutions of polydisperse polymers [1]. Their critical temperatures differ largely from the extrema of the two phase region so that τ changes its sign from positive to negative as one surpasses the critical temperature and approaches the homogeneous region of the system. For the same reason the correlation between σ and τ must fail for the present polydisperse copolymers. Theory considers the system to be homogeneous in case of $T > T_c$, in contrast to reality. Notwithstanding this situation, the correlation between σ and $\Delta\varphi$ remains reasonable [1].

Acknowledgements

We are indebted to S. Enders and M. Wünsch for their help with the computer calculations.

References

[1] Heinrich M, Wolf BA. Macromolecules 1992;25:3817–19.
[2] Heinrich M, Wolf BA. Polymer 1992;33(9):1926.
[3] Krause C, Wolf BA. Macromolecules 1997;30:885.
[4] Rätzsch MT, Wohlfahrt C. Adv Polym Sci 1990;98:51.
[5] Rätzsch MT, Kehlen H, Browarzik D, Schirutschke M. J Macromol Sci Chem 1986;A23(11):1349.
[6] Stockmayer WH. J Chem Phys 1945;13:199.
[7] Rätzsch M, Wohlfahrt C, Browarzik D, Kehlen H. J Macromol Sci Chem 1991;A28(1):47–64.
[8] Gibbs JW. Thermodynamics, 1. New Haven, Connecticut: Yale University Press, 1948.
[9] Stockmayer WH. J Chem Phys 1949;17:588.
[10] Rätzsch MT, Kehlen H, Bergmann J. J Macromol Sci Chem 1987;A24:1.
[11] de Gennes PG. Scaling concepts in polymer physics, London: Cornell University Press, 1979.
[12] Flory PJ. J Chem Phys 1942;10:51.
[13] Huggins ML. J Phys Chem 1942;46:151.
[14] Flory PJ. Principles of polymer chemistry, Ithaca: Cornell University, 1953.
[15] Ising E. Z. Physik 1925;31:253.
[16] Bondi A. J Phys Chem 1964;68:441.
[17] Gottlieb M, Herskowitz M. Macromolecules 1981;14:1468.
[18] Kambour RP, Bendler JT, Bopp RC. Macromolecules 1983;16:753.
[19] Enders S, Huber A, Wolf BA. Polymer 1994;35(26):5743.
[20] Binder K, Enders S, Wolf BA. J Chem Phys 1995;103(9):3809.
[21] Schneider A. PhD thesis, Mainz: Johannes Gutenberg-Universität, 1998.